Electronic Supplementary Material (ESI) for Nanoscale.
This journal is © The Royal Society of Chemistry 2019

Supporting Information - The Radiation Chemistry of Focused Electron-Beam Induced Etching of Copper in Liquids

Sarah K. Lami, Gabriel Smith, Eric Cao and J. Todd Hastings*

University of Kentucky, Department of Electrical and Computer Engineering, Lexington, Kentucky 40506, USA

Validation of Monte Carlo Simulations

Monte Carlo simulations in JMONSEL were validated by simulating the secondary electron (SE) yield of copper and of water as a function of primary electron energy. For copper, the carefully collected, ultra-high vacuum experimental results of Ding *et. al* were used as a reference.[2] Material parameters for copper were taken from Lin and Joy.[4] The comparison of the simulated and experimental SE yield is shown in Figure S1(a) with excellent agreement.

Three sources of experimental data for the secondary electron yield of water are available. Thiel *et al.* measured SE yield of bulk water in an environmental scanning electron microscope,[7] Suszcynsky *et al.* measured

*todd.hastings@uky.edu

the SE yield of water ice,[6] and Baglin *et al.* measured the SE yield of thin adsorbed water layers on Cu.[1] Figure S1(b), adapted from Joy and Joy's work,[3] plots these data sets along with our Monte Carlo simulation of bulk water. Good agreement was found for primary energies above 2 keV. Poorer agreement was observed for lower energies, but the experimental data is limited and diverges based on sample conditions. Transient charging that differs between bulk (Thiel) and adsorbed (Baglin) water may be responsible for these discrepancies.

Experimentally measured and simulated electron inelastic mean free paths (IMFP) in liquid water have been summarized in the recent paper by Nguyen-Truong.[5] The most recent simulations and experiments set an upper limit of $\approx$ 6 nm the IMFP of electrons between 1 and 2000 eV, and the IMFP is much smaller than 6 nm over much of this energy range. Thus, despite the divergence in the low energy results above, any error in calculating the range of these electrons is insignificant compared to the feature sizes and diffusion ranges considered here. Moreover, any change in radiolysis yield for these low energy energy electrons is already averaged into the measured radiation-chemical yields.

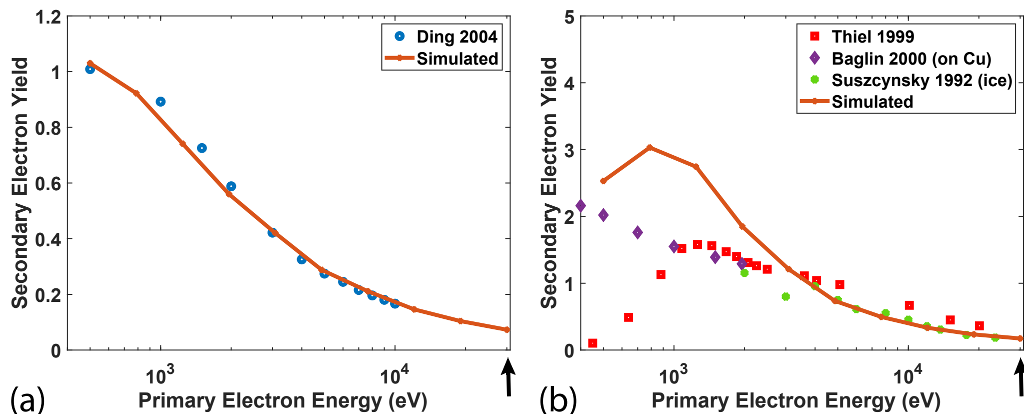

Figure S1: Validation of Monte Carlo simulations. (a) Comparison of simulated SE yield from copper with the data of Ding *et. al.* (b) Comparison of simulated SE from water with measured secondary electron yield from water,[7], ice[6] and adsorbed water on copper.[1] The plot of experimental data in (b) was adapted from reference 3. The 30 keV primary electron energy used in the experiments described here is marked with a vertical arrow.

Finite Element Simulation

The copper etching process was modelled by solving the continuity equation for the concentration of dilute species in the liquid volume and the movement of the liquid-solid boundary. We exploited the radial symmetry of the problem to reduce the simulation domain to two dimensions. This domain was given by the depth of the liquid with an 8 µm radius. The initial concentration for all chemical species were set to zero except for HSO_4^- which was set to 5 M to match experimental conditions. The boundary conditions were set such that the flux at the top boundary is zero. At the bottom boundary the

concentration of the oxidizing species was set to zero to reflect instantaneous etching of copper. The concentrations at the outer radial boundary were set to their initial values. Expanding the boundary beyond a radius of 8 µm changed the simulated etch volume by less than 0.001%.

The rates of reactions driven by the electron beam are given by

$$R_i(r,z) = \frac{G_i}{N_A}\frac{\Delta E(r,z)}{100}\frac{I_B}{q} \tag{1}$$

where $R_i(r,z)$ is the reaction rate of the ith species in mol m^{-3} s^{-1}, G_i is the radiation-chemical yield per 100 eV, N_A is Avogadro's number, $\Delta E(r,z)$ is the average energy absorbed per unit volume per primary electron in eV m^{-3}, I_B is the electron-beam current in amps, and q is the electron charge. G_i is negative for species undergoing radiolysis. $\Delta E(r,z)$ is calculated from the Monte Carlo model. The chemical reactions not driven by the electron beam are governed by the rates constants given in the main manuscript.

Diffusion was modelled by treating all species as dilute and using diffusion coefficients for infinite dilution. As noted in the main manuscript this approximation holds because the change in concentration, and the the diffusive flux, of the HSO_4^- remains small. We mapped the mesh so that it becomes coarser as one moves away from the beam impact point and the region of etching. The mesh was refined until there results changed by less than 0.01%. The size of the smallest and the largest mesh elements were 1 nm and 0.15 µm respectively.The simulation was carried out without considering

heat transfer.

The velocity of the liquid-solid (H_2SO_4(aq)-Cu) interface was determined by the normal flux of oxidizing species under the assumption that the electrodeposited copper had the same density as bulk copper. The vertical displacement of the boundary was constrained by the thickness of the copper layer. The layers below the electroplated copper were not included in the simulation. An example of how the etching process proceeds in time is shown in Fig. S2. The evolution of the concentration of ${S_2O_8}^{2-}$ and the moving liquid-solid interface can be seen at different time scales.

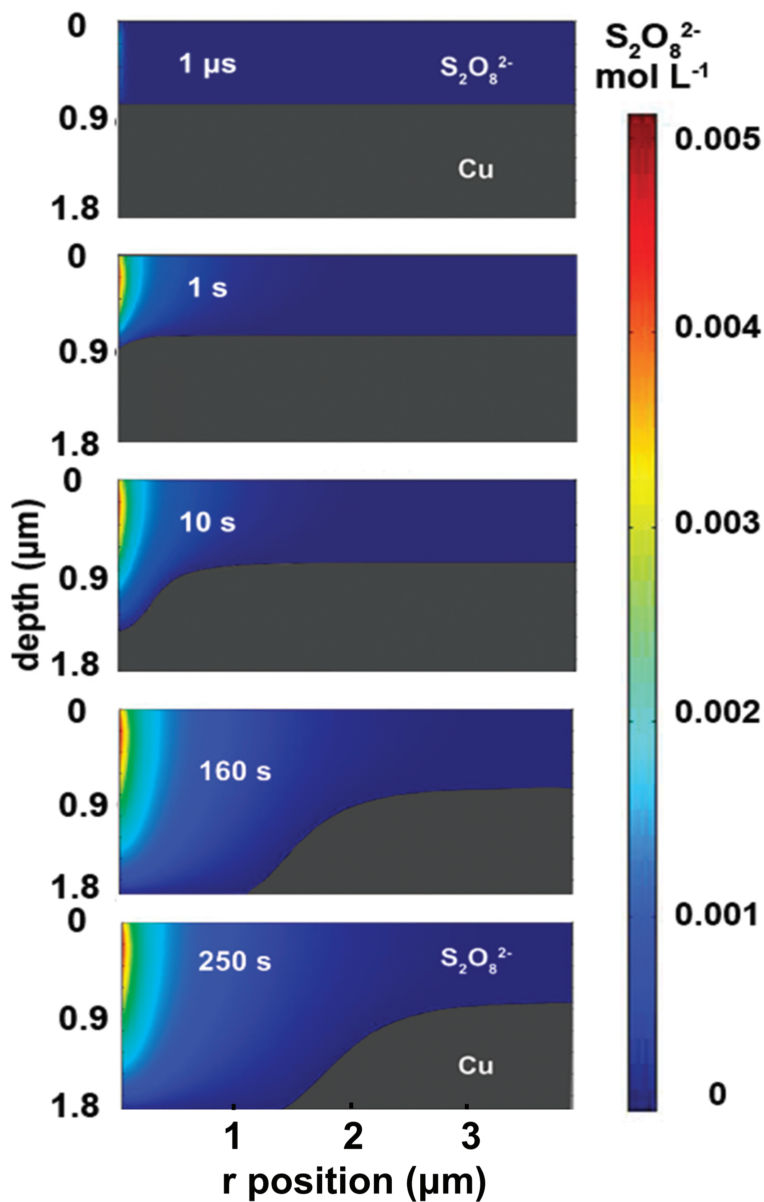

Figure S2: Hybrid simulation showing the time evolution of the Cu etching process and the concentration of $S_2O_8{}^{2-}$ when the solution is irradiated with 30 keV electrons, a 1 nA beam current, and 730 nm liquid thickness. Inset labels indicate the time point of each plot. The outer portion of the simulation domain (from 4 to 8 µm radius) is not shown to better resolve the concentrations and etched features.

References

[1] V Baglin, J Bojko, C Scheuerlein, Oswald Gröbner, M Taborelli, Bernard Henrist, and Noël Hilleret. The secondary electron yield of technical materials and its variation with surface treatments. Technical report, 2000.

[2] ZJ Ding, HM Li, XD Tang, and R Shimizu. Monte carlo simulation of absolute secondary electron yield of cu. *Applied Physics A*, 78(4):585–587, 2004.

[3] DC Joy and CS Joy. Scanning electron microscope imaging in liquids–some data on electron interactions in water. *Journal of Microscopy*, 221(2):84–88, 2006.

[4] Yinghong Lin and David C Joy. A new examination of secondary electron yield data. *Surface and Interface Analysis*, 37(11):895–900, 2005.

[5] Nguyen-Truong. Low-energy electron inelastic mean free paths for liquid water. *Journal of Physics: Condensed Matter*, 30(15):155101, 2018.

[6] David M Suszcynsky, Joseph E Borovsky, and Christoph K Goertz. Secondary electron yields of solar system ices. *Journal of Geophysical Research: Planets*, 97(E2):2611–2619, 1992.

[7] BL Thiel, D Stokes, and D Phifer. Secondary electron yield curve for liquid water. *Microscopy and Microanalysis*, 5(2):282–283, 1999.